Appl Phys A (2010) 100: 213–222
DOI 10.1007/s00339-010-5578-3

Applied Physics A
Materials Science & Processing

Carbon nanotube diameter tuning using hydrogen amount and temperature on SiO_2/Si substrates

M. Aksak · Y. Selamet

Received: 30 July 2009 / Accepted: 22 January 2010 / Published online: 12 February 2010

Abstract Carbon nanotubes (CNTs) were grown on thin iron (Fe) films on SiO_2/Si substrates by chemical vapor deposition (CVD) at four different hydrogen (H_2)/methane (CH_4) ratios at temperatures ranging from 925 to 1000°C. The effects of temperature and the amount of hydrogen gas on the mean diameter at increasing temperature were examined. We demonstrated that the mean diameter and its distribution depend not only on temperature but also on the H_2 amount. We showed that increasing H_2 amount strongly affects the structure of CNTs, especially at high growth temperature; the mean diameter at 1000°C reduced from about 383 to 34 nm by increasing H_2 amount from 24 to 50 sccm. We observed that at high temperature growth the mean diameter was decreasing very fast initially with increasing H_2 amount suggesting the dominance of H_2 over the growth temperature. A decrease in the slope of diameter vs. H_2 amount with further increment in H_2 amount implied that the temperature was, then, deciding the CNT diameter through catalyst particle coarsening. The statistical analysis presented implies that the H_2 amount has to be adjusted according to the growth temperature for given CH_4 amount to keep CNT diameter under control, and the large diameter distributions at high temperature and high H_2 amount can be associated with the large variation in the catalyst particle sizes.

M. Aksak · Y. Selamet (✉)
Carbon Nanostructures Laboratory, Department of Physics, Izmir Institute of Technology, 35430, Izmir, Turkey
e-mail: yusufselamet@iyte.edu.tr
Fax: +90-232-7507707

1 Introduction

The extraordinary properties of carbon nanotubes (CNTs) place them at the center of intense research and, hence, application fields for CNTs expand day-by-day. Scientifically, CNTs provide a rich quantum playground, while technologically they offer exciting alternatives to today's technology [1, 2]. On the other hand, the CNT growth process and dynamics are still not completely understood. CVD is a promising technique for CNT growth in terms of scalability to industrial needs and control over the growth parameters to some extent. Growth of CNTs by CVD is not an equilibrium process. The growth takes place at temperatures much lower than with the other two commonly used techniques for CNT growth, namely laser ablation and arc discharge. There is a wide range of parameters and large number of values associated with those for the CNT growth by CVD in the published literature, including some seemingly contradictory reports. This is mostly due to significant variation in the ideal growth conditions from system to system for effective CNT synthesis. Small, seemingly insignificant factors might change the end results to a large extent, leading to misinterpretation of data and wrong conclusions [3]. Failing to exactly repeat such secondary parameters leads to end results that vary considerably. Nonetheless, a number of H_2 to hydrocarbon (C_nH_m) ratios exist at given temperatures and pressures, leading to more efficient growth and lessening the consequences of other parameters.

We studied CNTs grown on silicon dioxide/silicon (Si/SiO_2) substrates. It has been shown that CNTs grown on aluminum oxide (Al_2O_3) with Fe a few nanometers thick in ethylene CVD yield densely populated and vertically aligned CNTs [4]. However, direct growth on SiO_2/Si is very important since it allows integration of CNTs with microelectronics technology and opens the possibility of ben-

efiting from already very advanced silicon processing technology [5–7].

During CVD growth of CNTs with C_nH_m gasses, at least one carrier/dilute gas is used to prevent formation of amorphous carbon around nano-sized catalyst particles, which makes the catalyst particles inactive. The carrier/dilute gas also helps to regulate growth kinetics by adjusting decomposition rate of the C_nH_m gas [8]. H_2 is the preferred supplementary gas; however, other gasses such as nitrogen, argon, oxygen, helium, and ammonia have also been used with or without H_2 [9–11]. H_2 is used to both arrange the reaction kinetics and to help form catalyst material into shapes that catalyze CNTs [12, 13]. H_2 also keeps catalyst particles alive by removing amorphous carbon deposits [14] and surface carbide [15], both make metal particles inactive to catalyze. While most studies reported that supplementary H_2 was very useful in CNT growth [16], some others disagreed. For example, a recent report questioned the role of supplementary H_2 in CVD growth, claiming that H_2 coming from C_nH_m decomposition would yield more efficient CNT growth, with supplementary H_2 added later, towards the end of the process [17]. Another work reported that hydrogen radicals can have deleterious effects on Single Walled CNTs (SWNT) growth by plasma enhanced CVD, etching away grown NT structures and hence, hindering the growth process [18]. This study reported that when only H_2 was added to CH_4 that CNTs grew to be only scarcely populated. In this report it was claimed that oxygen was needed in addition to H_2 for a vertically aligned growth, which annihilated the effects of H_2 before it destroyed the tubular structure. Other works report that oxygen etches away both amorphous carbon and carbon in the CNT structure [18, 19] if used in too great a quantity. Oxygen has been used widely to open up the rounded hemispherical fullerene ends of SWNTs [20]. Another study reported that a small and controlled amount of H_2O vapor keeps the catalyst free from amorphous carbon [21]. It was claimed that oxygen was too strong an oxidizer, oxidizing, or worse, burning nanotubes along with amorphous carbon; therefore, a weak oxidizer, such as H_2O vapor along with H_2, was recommended [22]. However, for H_2O vapor to work, a small amount with a very narrow relative amount range (150–200 ppm) had to be used, or CNT growth was significantly suppressed [23]. Another work reported that both H_2 and oxygen promote high crystalline CNT growth [24]. In all of the above studies, H_2 was the main constituent and it appears as if it is the indispensable element in CNT growth by CVD. Therefore, the question is, what is the right amount of H_2 in proportion to the C_nH_m? The effects of H_2/CH_4 ratio have been studied in the past [25, 26]. However, most of the research was either on supported catalysts embedded in the support matrix with predetermined particle sizes, or it lacked to scan both temperature and the H_2/CH_4 ratio regimes.

In this work, we planned experiments to study the influence of H_2 in CH_4-CVD on the growth of CNTs grown on thin Fe films sputtered on SiO_2/Si substrates. Four different H_2/CH_4 ratios were studied at four different growth temperatures. Growth runs did not follow any particular order to exclude possible growth memory effects and also to single out any experimental errors. Based on previous experience, we found that a CH_4 flow of 100 standard cubic centimeters per minute (sccm) gives relatively better results when combined with a H_2 flow of 50 sccm. However, at these conditions, H_2 levels above 50 sccm resulted in CNTs with poor structural quality. Therefore, we started the investigations at the optimal H_2 content, 50 sccm, and lowered the H_2 amount in the H_2/CH_4 ratio. The results of this work show that H_2 and its ratio to CH_4 play a very important role in CVD growth, and that role is temperature dependent. We observed a very large increase in the mean diameter at low H_2 content at high temperatures, which emphasizes the importance of the supplementary H_2 and might be of great interest since this work shows how to control the diameter at those extreme conditions.

2 Experimental

In this work, we first employed a magnetron sputtering system to deposit very thin Fe films on commercially purchased SiO_2/Si substrates. The chamber base pressure was 1×10^{-6} Torr prior to catalyst film growth. The substrates were cleaned chemically in methanol for 15 min in an ultrasonic bath and rinsed with ultra-pure water for 15 min prior to growth. The depositions were carried out in DC sputtering at 20 W, with a growth rate of 0.1 Å/s, measured by a thickness monitor, at a growth pressure of 0.5 mTorr. The Fe catalyst film thickness was calculated from the growth rate as approximately 3.5 nm. The samples used in this study were scribed from the same larger substrate before the CNT growth. The samples were kept under vacuum conditions until the time of CNT growth to protect their surface from contamination and further oxidation. The CVD system used for this study was evacuated by a mechanical pump down to mTorr scale. The system was continuously kept under vacuum while not in use, and high purity argon (Ar) flow was used to bring it to the atmospheric pressure for sample loading. After reaching sufficiently low vacuum, the temperature was set to the growth temperature with a increase rate of about 30°C/min. The Ar flow was kept constant at 120 sccm until the given growth temperature was reached. The samples were subjected to H_2 pretreatment at 120 sccm before introducing CH_4. Flow rate of the gases was controlled by electronic mass flow meters. For CNT growth, we used CH_4/H_2 with four different flow rates for 30 minutes under system pressure of ~350 Torr. The growth was terminated by turning off CH_4 flow and the samples were allowed

to cool down to room temperature under Ar gas flow. We characterized our as-grown CNTs by Scanning Electron Microscope (SEM) (Phillips XL-30S FEG) to study their morphology and to obtain the length and diameter of these as-grown CNTs. For some of our samples, Raman spectroscopy measurements were utilized for obtaining the crystallinity and structure of CNTs. The Raman images were taken with a Renishaw micro-Raman 2000 with 632.8 nm line of a He–Ne laser. Energy dispersive X-ray (EDX) measurements along with XRD (Philips X'pert Pro X-ray diffractometer with Cu-K_α X-ray source $\lambda = 1.5418$ Å) scans were also carried out to investigate the elemental and crystal composition of our samples.

3 Results and discussion

At higher temperatures surface roughness increases due to de-oxidation of the surface [27] or due to thermal expansion coefficient mismatch between the layers [28]. It is generally accepted that there is a strong correlation between the size of the catalyst particle and CNT diameter [29, 30]; however, it is still under debate what controls the size of the catalyst particles when thin film catalyst is used to synthesize nanotubes. There were reports that the thickness of the film [3, 31]; pretreatment conditions [17], including plasma etching, gas treatment time; and temperature [32] play an important role in the size of the catalyst particles. From our experience we know that at high growth temperatures catalyst particles become rather large [33]. The enlargement in the particle size is most likely due to fact that at high temperatures, metal oxide loses its oxygen and becomes elemental; a catalyst metal without oxygen, especially on a SiO_2 surface, coalesces more easily and forms larger nanoparticles [4]. However, larger particles are less effective in catalyzing nanotubes [33]. The amount of H_2 is the key to deciding the final diameter of CNTs since it reduces the metal oxide films and adjusts reaction kinetics. To understand how H_2 affected the diameter under our growth conditions, SEM images of CNTs at different magnifications and at several locations for each sample were taken. It is known that high temperature growth improves the crystal quality of the CNTs [34, 35]. In our experience we have also found that temperatures below 850°C are too low to effectively synthesize CNTs using CH_4 on thin film catalysts. Similar works have reported that higher growth temperature yields more effective synthesis with CH_4 [36, 37]. We performed several experiments with the ratio of H_2 to CH_4 of 50:100, 40:100, 34:100, and 24:100 at a temperature range of 925–1000°C. Figures 1–4 display the representative SEM images of CNTs grown at 925, 950, 975, and 1000°C, respectively. In each figure we show from (a)–(d) the different ratios of H_2 to CH_4, 50 : 100, 40 : 100, 34 : 100, and 24:100, respectively. Sample names, indicating the growth sequence and the mean, standard deviation and standard error of the mean of the diameters obtained from SEM images are summarized in Table 1. The statistical diameter distributions were mostly skewed right (14 out of 16 samples), imitating log-normal distribution which suggest particle migration and coalescence growth [38]. The reported results were obtained from large numbers of SEM pictures, resulted in very small

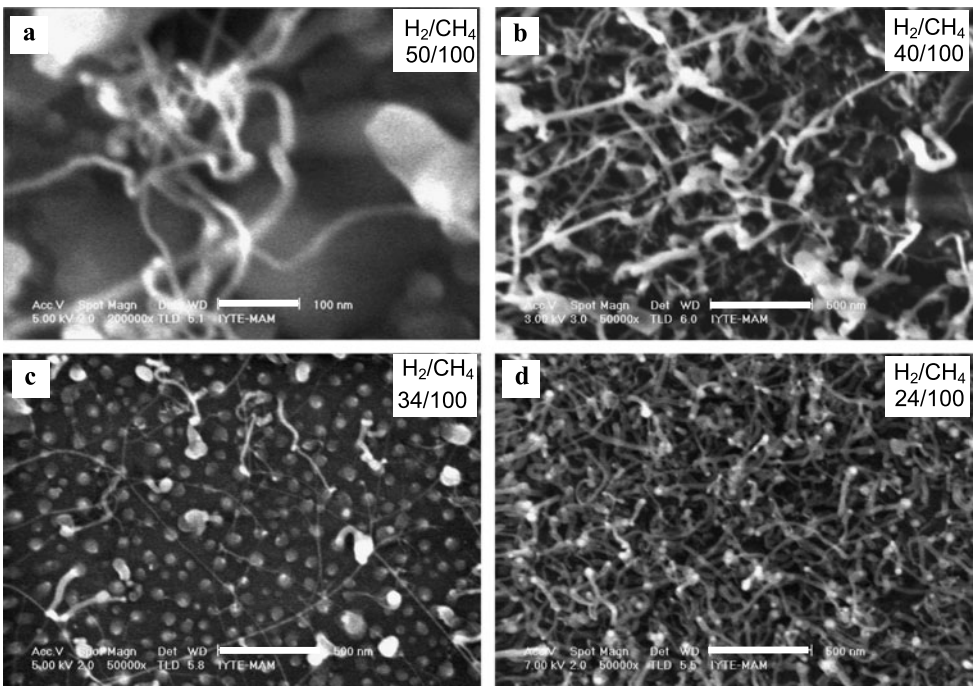

Fig. 1 SEM pictures of samples grown at 925°C with H_2/CH_4 ratios (sccm) given on the pictures (**a**) cnt57, (**b**) cnt66, (**c**) cnt69, (**d**) cnt72. Scale bars: (**a**) 100 nm, (**b–d**) 500 nm

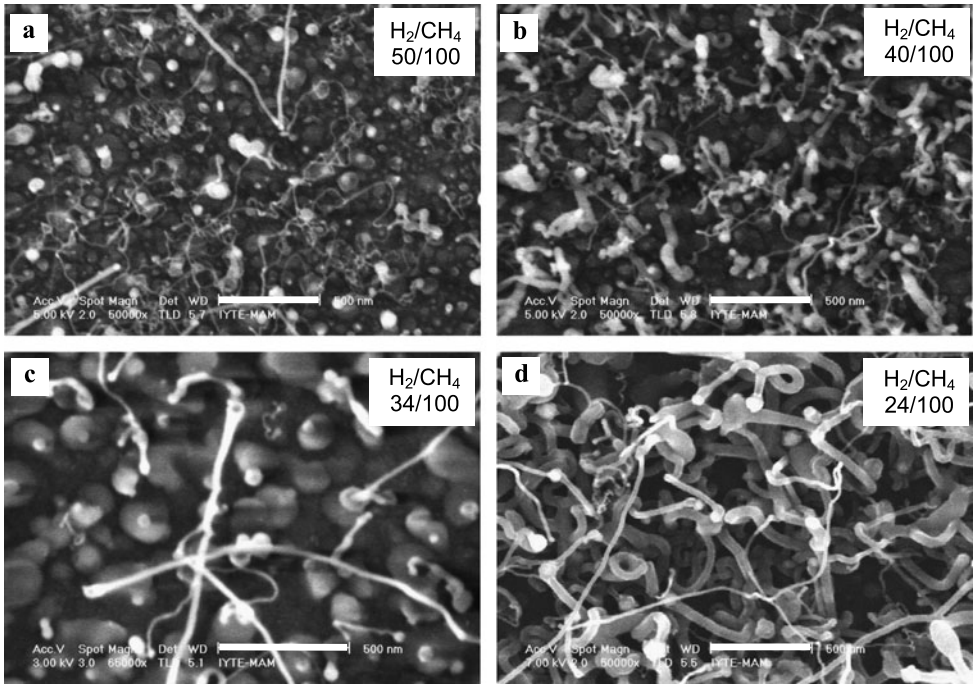

Fig. 2 SEM pictures of samples grown at 950°C with H_2/CH_4 ratios (sccm) given on pictures (**a**) cnt62, (**b**) cnt64, (**c**) cnt70, (**d**) cnt73. Scale bars: (**a**–**d**) 500 nm

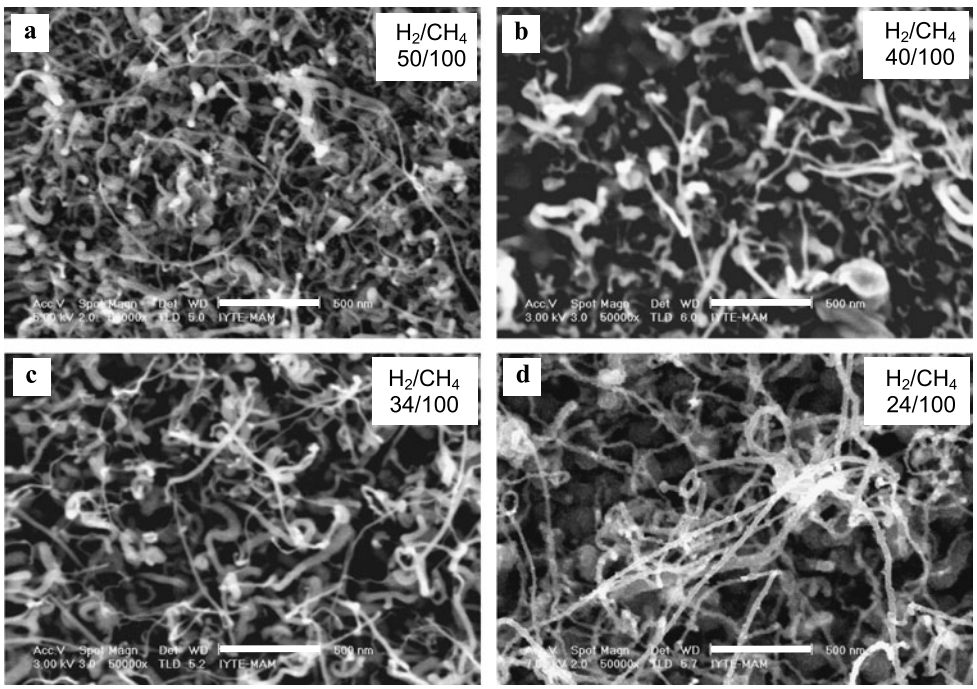

Fig. 3 SEM pictures of samples grown at 975°C with H_2/CH_4 ratios (sccm) given on the pictures (**a**) cnt59, (**b**) cnt67, (**c**) cnt71, (**d**) cnt74. Scale bars: (**a**–**d**) 500 nm

standard errors. A small standard error of mean diameter implies that adding more diameter measurements to sum would only increase number of counts while standard deviations remaining the same. For the diameter study, we first grew CNTs with 50:100 sccm H_2:CH_4 ratio, shown in Fig. 1a. We found that the mean diameter of these as-grown CNTs was approximately 14.5 nm, whereas the mean diameter of as-grown CNTs was found to be nearly 21.0 nm when we used 40:100 sccm (Fig. 1b). However, when the H_2 ratio was decreased to 34 sccm, we observed that the mean diameter of as-grown CNTs decreased to 11.3 nm (Fig. 1c), while the mean diameters changed to 17.6 nm when we decreased the ratio of H_2 to CH_4 are further to 24:100 (Fig. 1d). SEM images also revealed that CNTs were grown in a tangled mode, whereas at high temperature and at low H_2 ratios, CNTs were grown vertically (Figs. 4c and d), which is usually due to crowding. We also performed EDX characterizations on the samples to confirm the CNT formation and pres-

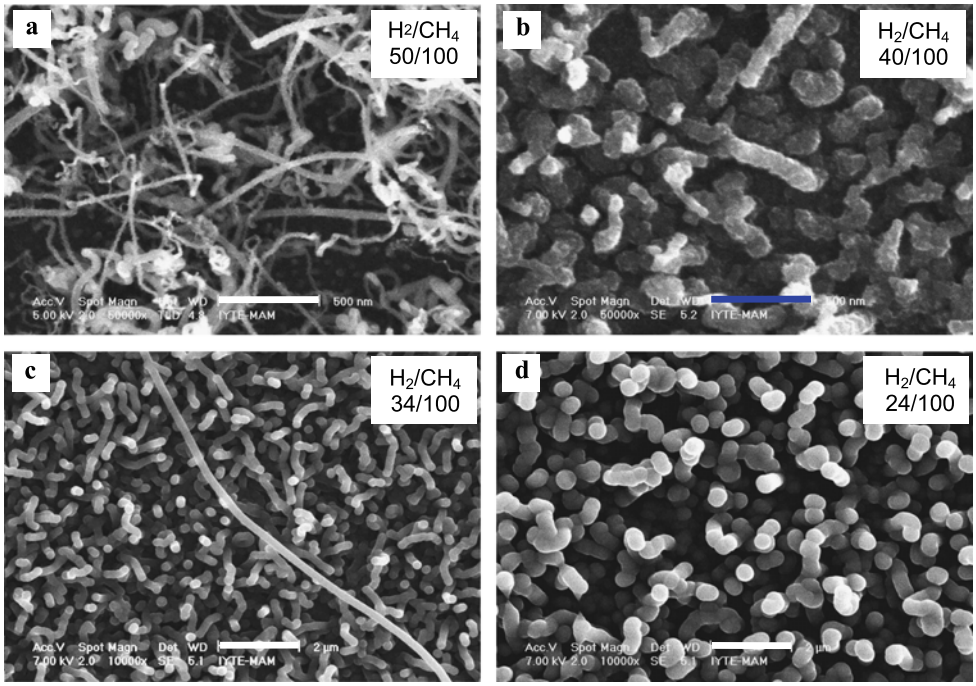

Fig. 4 SEM pictures of samples grown at 1000°C with H_2/CH_4 ratios (sccm) given on the pictures (**a**) cnt60, (**b**) cnt68, (**c**) cnt65, (**d**) cnt61. Scale bars: (**a**, **b**) 500 nm, (**c**, **d**) 2 μm

Table 1 List of the samples studied at given growth conditions and the mean diameters (d_{mean}) obtained in this study. SD stands for standard deviation and SEM stands for standard error of mean diameter

H_2	925°C				950°C				975°C				1000°C			
	Sample name	d_{mean} (nm)	SD	SEM	Sample name	d_{mean} (nm)	SD	SEM	Sample name	d_{mean} (nm)	SD	SEM	Sample name	d_{mean} (nm)	SD	SEM
Amount (sccm)																
50	CNT57	14.5	8.4	1.1	CNT62	13.0	3.3	0.5	CNT59	19.6	8.4	1.0	CNT60	34.3	13.3	1.3
40	CNT66	21.0	4.8	0.5	CNT64	16.7	5.8	0.7	CNT67	23.6	4.4	0.5	CNT68	84.7	25.3	3.4
34	CNT69	11.3	5.6	0.8	CNT70	18.3	3.5	0.5	CNT71	18.7	8.3	0.9	CNT65	188.7	11.9	1.4
24	CNT72	17.6	4.2	0.5	CNT73	32.5	12.9	1.4	CNT74	23.2	5.2	0.6	CNT61	383.2	41.2	5.4

ence of the catalyst particles. It was seen from this analysis that the Fe concentration was highest at the tips, which led us to conclude that the CNTs were grown according to tip growth mechanism. In the tip growth mechanism catalyst particle rises up with growing CNT and, hence, has size directly related to the CNT inner diameter.

H_2 amount had a substantial effect on diameters at high temperature. Increasing H_2 amount was very effective in reducing diameters; at this temperature increasing H_2 amount yielded smaller diameters, however, its effectiveness was decreasing with H_2 amount (Fig. 5). There was a gradual decrease in the diameters at the temperatures of 925 and 975°C with increasing H_2 amount (Fig. 5 inset), although this was not as dramatic as the one we observed at the high temperature. The observed behavior at 950°C was very similar to the one observed at high temperature; a fast initial decrease followed by slow decrease in diameters with increasing H_2 amount. High temperature growth is also distinct with respect to strong dependence on H_2 amount. At temperatures lower than 1000°C, changes in the diameter were comparatively small. On the other hand, without exception all samples showed large increases in diameters at 1000°C. From examining the diameter vs. H_2 rate plot at lower temperatures (Fig. 5 inset) we saw that for 50/100 and 40/100 rates, diameter rank from larger to smaller at growth temperatures 975, 925 and 950°C did not change. However, at lower H_2 rates (34/100 and 24/100), the mean diameters obtained at 950°C growth first exceeded the diameters obtained at 925°C growth, then surpassed the diameters obtained at 975°C growth, becoming the largest diameter at the least H_2/CH_4 ratio. This suggested to us a correlation between H_2/CH_4 ratio and the growth temperature. For that reason, we looked at variation of CNT diameter with temperature for given H_2/CH_4 ratio (Figs. 6a–d). We observed that at lower

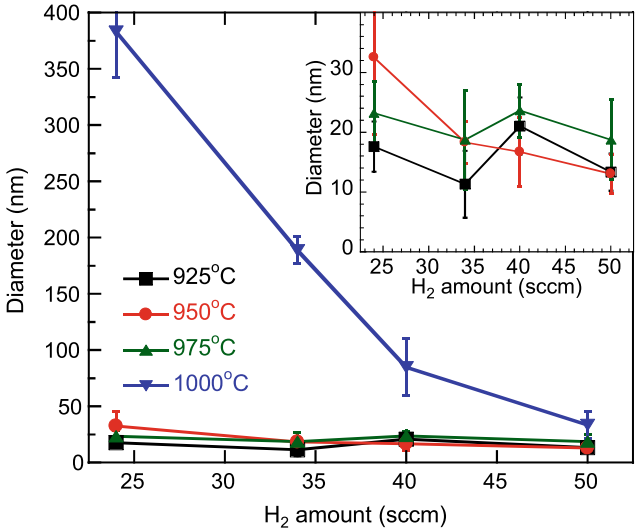

Fig. 5 Variation of mean diameter with H_2 amount while CH_4 amount was kept at 100 sccm. Inset shows the mean diameter values at lower temperatures 925–975°C in detail. Standard errors of the mean diameter obtained are less than the symbol sizes. 95% confidence intervals were larger than symbol sizes only at high temperature (1000°C) and/or at high H_2 amount (50 sccm) data. The *error bars* shown are the ± standard deviations of the diameters

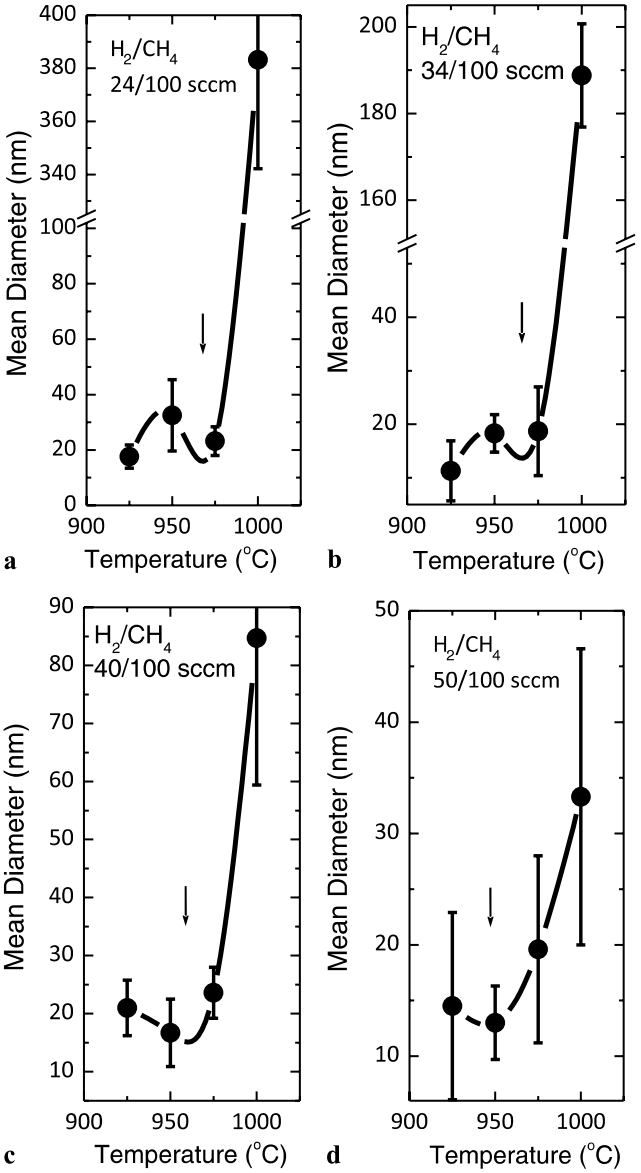

Fig. 6 Mean diameter variation as a function of growth temperature. (**a**) H_2/CH_4: 24/100 sccm, (**b**) H_2/CH_4: 34/100 sccm, (**c**) H_2/CH_4: 40/100 sccm, (**d**) H_2/CH_4: 50/100 sccm. *Solid curves* are the B-spline fits to data. The *error bars* in the figures are the ± standard deviations of the diameters. Note the break in *y* axis in (**a**) and (**b**). For the explanation of the *arrows* see text

H_2 ratio (Fig. 6a), mean diameter varied rather erratically with temperature, which implied that growths at this ratio would be difficult to control, and further that it would be difficult to guess the outcome from the beginning. The next ratio, 34/100, showed a similar behavior. However, this time variation was less erratic. As the ratio increased, CNT diameter varied more steadily, which would make growths at this ratio preferred. In addition, the shapes of the curves obtained by basis spline (B-spline) interpolation to data showed a quite noticeable transition; the wavy nature damped with the increasing temperature. Care must be taken interpreting the curves, since considering a single graph might be misleading. We used this interpolation to compare temperature dependent behavior when H_2 amount changed. Using this interpolation, the minima that we observe lowering temperature from 1000°C, shifts from about 969°C for 24/100 ratio, to 966°C for 34/100 ratio, to 959°C for ratio 40/100, and to 945°C for ratio 50/100. The arrows marking the location of the minima in Figs. 6a–d clearly shift toward lower temperatures with increasing H_2 amount. Looking at the two highest temperature ratio (1000/975) plotted against H_2 amount together with the minima, we saw that there was a correlation (Fig. 7), which implied that how fast the diameter is plunging down related to the location of the minimum. The observed difference between these two data sets is due to alignment of the mean diameters at 925 and 950°C compared to 975 and 1000°C (see Figs. 6a–d).

The diameter at high temperature more than doubling in each step increased from about 34 to 383 nm when H_2 amount decreased from 50 to 24 sccm, respectively (Table 1). This is due to differences in both H_2 amount and H_2/CH_4 ratio. The difference can be clearly seen from the normalized diameter plot (Fig. 8). From that graph we observe a clear dependence on the temperature and the data was lining up with the H_2 amount. H_2 amounts 50 and 40 sccm showed similar behavior with the temperature; the diameters increasing at the final temperature (925°C) while H_2 amounts 34 and 24 showed almost identical change with the temperature; the diameters decreasing at the final temperature (925°C) when reduced from highest temperature.

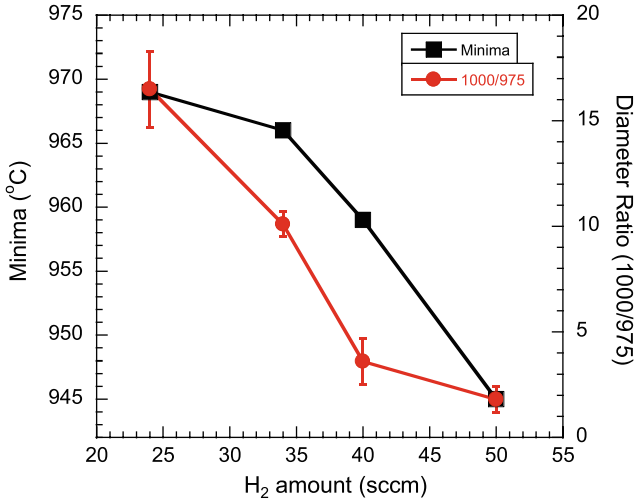

Fig. 7 The first minima observed in the mean diameters as the growth temperature reduced from 1000°C. The diameter ratio of two neighboring temperatures is also plotted on right axis along vs. H_2 amount. The *error bars* are the ± standard deviations

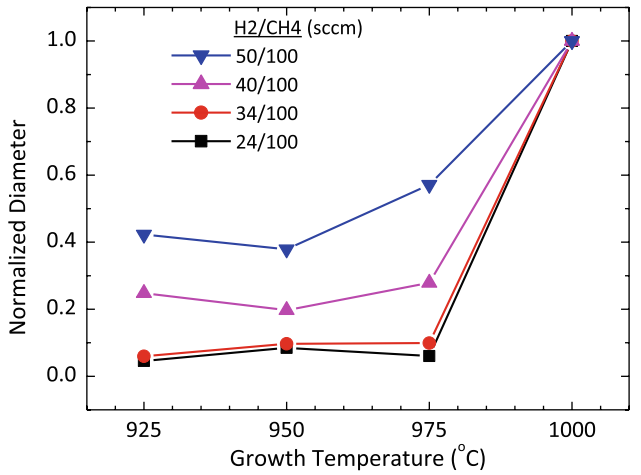

Fig. 8 Normalized plots of the mean diameters vs. the growth temperature. The *solid lines* are drawn to guide the eyes

Considering increases observed in the mean diameters at the high temperature (Table 1) the observed differences in normalized plot is due to changes in H_2 amount and in part due to changes in H_2/CH_4 ratio. From the normalized plot we can see that a gradual increase in the diameter with temperature for H_2 amount of 50 sccm should be chosen as optimal rate for the easy diameter control in CNT growth for the whole temperature range, whereas in the other H_2 amounts, increasing temperature from 975 to 1000°C would result in very large increases in diameters. H_2 amount of 50 sccm led to variations in diameters, i.e. the standard deviations, comparable to the other amounts; however, within the diameter measurement range the variations (error bars in Fig. 6d) were larger than the other ranges (Figs. 6a–c). This increase in the distributions at the high temperature was attributed to reduction of Fe films followed by coalescence.

The temperature, catalyst film thickness and H_2 amount decide the catalyst particle diameter and closely related CNT diameter. The catalyst film thickness (3.5 nm) was larger than thicknesses normally used, which allowed us to have larger diameters by supplying enough material. When H_2 amount is not enough during growth at high temperatures, amorphous carbon accumulation starts over CNTs. The separation between the lines connecting data points in Fig. 8 were decreasing with the decreasing H_2 to CH_4 ratio suggesting the ratios are not optimal so that the diameters show no sign of difference. In the temperature region of 975 to 1000°C the supplied heat is sufficiently high for self-pyrolysis, allowing more than enough carbon stock from CH_4, which also leads to amorphous carbon deposition. As observed from Fig. 8, an increased amount of H_2 would lessen these consequences.

There have also been reports that the enlargement in CNT diameter might be due to larger catalyst sizes and amorphous carbon covering of nanotubes using less stable C_nH_m supplies [39–41]. It is known that CH_4 is the most stable hydrocarbon, which makes it the carbon source that goes to self-pyrolysis at the highest temperatures [42, 43]. In studies of high temperature methane CVD growth at 1000°C using supported catalyst Kong et al. [44] and Kang et al. [45] obtained CNTs without H_2 and with H_2, with diameters in quite a small range (1–6 nm) and (10–15 nm), respectively. Kong et al. reported scarce amount of amorphous carbon, while Kang et al. stated substantial amorphous carbon observations in space among the tubes. Kong et al. attributed their amorphous carbon free growth to short growth time (10 min) and very large CH_4 flow rate (6150 sccm). Biris et al. studied the H_2/CH_4 dependence at single growth temperature of 850°C and found a weak dependence of CNT diameter to this ratio [26]. Nevertheless, none of these groups reported any amorphous carbon deposition over CNTs, enlarging their diameters. The diameter enlargements similar to ours were observed with CNT growths using thin film catalysts at high temperatures using CH_4 [46, 47]. However, no discussion was raised over those large diameter results other than simply assuming that the enlargement was due to amorphous carbon deposition over CNTs. Most of the publications state that amorphous carbon deposition was moderate in growths using CH_4 as the carbon source, making the enlargement observed in diameter be most probably due to catalyst particle coarsening at high temperatures. This enlargement might be the result of de-oxidation of metal oxide due to high temperatures or H_2 reduction A substrate such as SiO_2 can also provide a platform to already formed particles where they can move very fast and easily coalesce into even larger particles, however, this cannot explain H_2 dependence we observed. The strong H_2 dependence at high temperature

is due to, the important role H_2 assumes. The enlargement in the CNT diameter is due to autocatalytic decomposition of CH_4 at higher temperatures and deposition over the CNT and substrate surfaces as a non-graphitic carbon. Reducing the H_2 amount adds to the thickening due to amorphous carbon deposition since disproportionation reaction equilibrium, then, will be decided by CH_4 [25]. At low temperatures the CH_4 decomposition is through the catalyst particle leading to smaller diameter CNTs, since at low temperatures the catalyst particles are also remaining small. At high temperatures, however, the CH_4 decomposition is mostly through self-pyrolysis, yielding growth with very large diameter CNTs. This scheme can successfully explain the H_2 ratio dependence observed in Fig. 8; i.e., smaller diameter changes at higher H_2 rates (50 and 40) compared to those at lower H_2 rates (34 and 34 sccm). This analysis shows that the contribution of H_2 to CNT growth is more prominent than most have assumed, especially at high temperatures. This scenario can also explain the reports that CNTs did not grow efficiently without H_2 presence [12, 48]; if metal oxide is not reduced, catalyst particles do not easily form and without right amount of H_2 there will be amorphous carbon coverage. Large diameters observed at high temperature and low H_2 amount likely due to non-graphitic carbon covering over the structures. That thickening is due to uniform deposition and must lead to narrow thickness distribution. Therefore, the large diameter distributions at high temperature must be due to large variation in the catalyst particle sizes.

For some of our samples, Raman spectroscopy measurements (He-Ne laser, 633 nm, on a 2 μm^2 area) were utilized to see how the growth temperature affects the CNT quality. The Raman spectra of CNTs grown at 950°C with 50:100 H_2:CH_4 ratio point to the presence of SWNTs (Fig. 9a). The CNTs grown at 950°C with 50:100 ratio were of very high purity, as indicated in the spectra by very low intensity of D-band around 1300 cm^{-1}, and by very narrow G-band at 1594 cm^{-1}, which had a shoulder at 1558 cm^{-1}, strongly indicating the abundance of semiconducting SWNTs. No RBM peaks were observed, which was attributed to the diameters being larger than 3 nm [49]. CNTs grown at 975°C with 50:100 had inferior quality to those grown at 950°C (Fig. 9b). The Raman spectra have higher intensity of D-band (at 1335 cm^{-1}) than that of G-band (at 1580 cm^{-1}), along with the broadened D-band with a full width at half maximum (FWHM) of about 60 cm^{-1}. This broadening and higher intensity may be the result of several D-bands due to amorphous carbon and defective graphitic structures overlapping [50]. The Raman measurements taken from different points on the sample named CNT59 yielded consistent I_D/I_G ratio of about 2.3 (Fig. 9b). Observed D-band increase in the Raman spectra with increasing temperature might also be accounted for by non-graphitic deposition over CNTs.

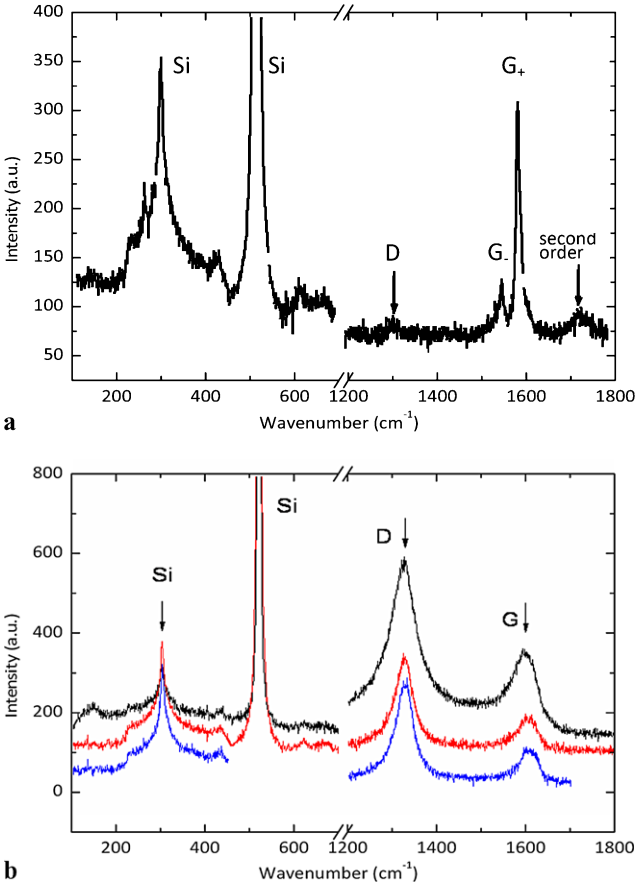

Fig. 9 Raman spectra of as-grown carbon nanostructures grown under H_2:CH_4 50:100 (sccm) ratio and at temperature of (**a**) 950°C and (**b**) 975°C

The publications we mentioned above using thin film catalyst presented two SEM images that support our findings [46, 47]. Hart et al. published an SEM picture of fibrous structures with diameters larger than a micrometer in CH_4 growth of CNT on Mo/Fe/Al_2O_3/Si at 1025°C [46]. In that work, fibrous growth at H_2/$CH_4$40/360 sccm ratio was achieved at 1025°C. We calculated the average diameter of their CNTs using their published SEM picture as 1.2 μm. The other work reports very large diameters (calculated to be ∼4.5 μm from their SEM pictures) of CNTs grown at 1100°C on Si substrate with Fe film deposited prior to the growth [47]. We plotted these two results with large diameters together with our high temperature results in Fig. 10. The agreement of the data, even without considering effects such as total flow, pressure, etc., was quite notable. Increasing the total flow rate, for example, at the same H_2/CH_4 ratio might have had increased CNT yield, usually not affecting diameter. This agreement shows the universality of the process which leads to larger diameters.

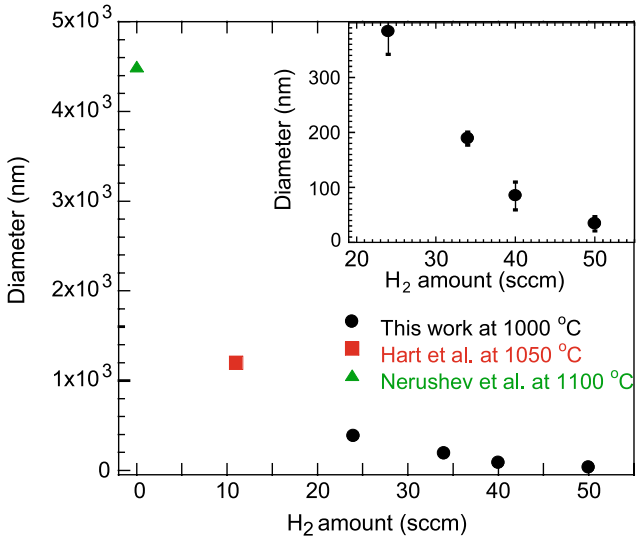

Fig. 10 Mean diameters of the growth at high temperature vs. H_2 amount (sccm) including two results obtained from literature. *Inset* re-plots the results obtained in this study for comparison

4 Conclusions

We studied the diameters of CNTs grown on Fe/SiO_2/Si by varying H_2/CH_4 ratio and growth temperature. Strong H_2 amount and H_2 to CH_4 ratio dependence of the diameter was observed especially at high temperature; all ratios showed large increase in diameters. The mean diameters were decreased fast with increasing H_2 amount. However, increasing H_2 amount to 50 sccm spread the diameter distribution. At low temperatures CNT diameters were varying within some narrow margin with similar H_2/CH_4 ratio dependence. There was a parallel between the dip observed at diameters as the growth temperature reduced and the observed large diameters at high temperature growth. At high temperature, the mean diameter was decreasing very fast and leveling off with increasing H_2 amount suggesting the dominance of H_2 over the growth temperature. Decreased slope suggest that temperature is, then, key parameter in deciding the diameter at right H_2 amount through catalyst particle coarsening. Our analysis explains the large diameters observed in the literature at extreme conditions of high temperature and low/none hydrogen amount. We found that it was easier to control CNT diameter at higher H_2 content than that at lower H_2 content. Out of the studied parameters we found that best conditions to growth CNTs were at 950°C and a 50/100 sccm H_2/CH_4 ratio. Under growth conditions of high temperature and insufficient H_2 amount, the enlargement observed on the CNT diameters can be attributed to amorphous carbon coverage due to increased self-pyrolysis of CH_4 as suggested also by the Raman analysis. The large diameter distributions at high temperature and high H_2 amount can be associated with the coarsening of the catalyst particles and large variation in the particle sizes. This work demonstrates that H_2 in CVD growth is very important; it can be used to adjust the diameters at given CH_4 rate at high temperatures where self-pyrolysis takes place, and at lower temperatures where high quality CNT is needed.

Acknowledgements This study was supported by The Scientific and Technological Research Council of Turkey project no. 105T462. We are very thankful to Prof. Anne Marie Bunnot of CNRS, Grenoble, France for measuring Raman shifts of several samples. We also thank Serap Kir for some technical help, Suleyman Tari for the growth of Fe film by sputtering, H. Kreuzer for her suggestions on the manuscript, and IYTE Material Research Center for SEM pictures.

References

1. P. Avouris, Phys. Today **62**, 34–40 (2009)
2. S. Frank, P. Poncharal, Z.L. Wang, W.A. de Heer, Science **280**, 1744 (1998)
3. T. Yamada, T. Namai, K. Hata, D.N. Futaba, K. Mizuno, J. Fan, M. Yudasaka, M. Yumura, S. Iijima, Nat. Nanotechnol. **1**, 131–136 (2006)
4. C. Mattavi, C. Wirth, S. Hofmann, R. Blume, M. Cantoro, C. Ducati, C. Cepek, A. Knop-Gericke, S. Milne, C. Castellarin-Cudia, S. Dolafi, A. Goldoni, R. Schloegl, J. Robertson, J. Phys. Chem. C **112**, 12207–12213 (2008)
5. G.S. Duesberg, A.P. Graham, M. Liebau, R. Seidel, E. Unger, F. Kreupl, W. Hoenlein, Nano Lett. **3**, 257–259 (2003)
6. W.H. Teh, C.G. Smith, K.B.K. Teo, R.G. Lacerda, G.A.J. Amaratunga, W.I. Milne, M. Castignolles, A. Loiseau, J. Vac. Sci. Technol. B **21**, 1380–1383 (2003)
7. J.M. Simmons, B.M. Nichols, M.S. Marcus, O.M. Castellini, R.J. Hamers, M.A. Eriksson, Small **2**, 902–909 (2006)
8. N. Yoshida, T. Yamamoto, F. Minoguchi, S. Kishimoto, Catal. Lett. **23**, 237 (1994)
9. M. Jung, K.Y. Eun, J. Lee, Y. Baik, K. Lee, J.W. Park, Diam. Relat. Mater. **10**, 1235 (2001)
10. T.Y. Kim, K.R. Lee, K.Y. Eun, K.H. Oh, Chem. Phys. Lett. **372**, 603–607 (2003)
11. Z.F. Ren, Z.P. Huang, J.W. Xu, J.H. Wang, P. Bush, M.P. Siegal, P.N. Provencio, Science **282**, 1105–1107 (1998)
12. A.G. Nasibulin, D.P. Brown, P. Queipo, D. Gonzalez, H. Jiang, A.S. Anisimov, E.I. Kauppinen, Phys. Status Solidi B **243**, 3095–3100 (2006)
13. F.B. Rao, T. Li, Y.L. Wang, Physica E **40**, 779–784 (2008)
14. L. Dong, J. Jiao, S. Foxley, D. Tuggle, C.L. Mosher, G.H. Grathoff, J. Nanosci. Nanotechnol. **2**, 155–160 (2002)
15. L. Ci, Y. Li, B. Wei, J. Liang, C. Xu, D. Wu, Carbon **38**, 1933–1937 (2000)
16. G.Y. Xiong, Y. Suda, D.Z. Wang, J.Y. Huang, Z.F. Ren, Nanotechnology **16**, 532–535 (2005)
17. G.D. Nessim, A.J. Hart, J.S. Kim, D. Acquaviva, J. Oh, C.D. Morgan, M. Seita, J.S. Leib, C.V. Thompson, Nano Lett. **8**, 3587–3593 (2008)
18. G.Y. Zhang, D. Mann, L. Zhang, A. Javey, Y. Li, E. Yenilmez, Q. Wang, J.P. McVittie, Y. Nishi, J. Gibbons, H. Dai, Proc. Natl. Acad. Sci. **102**, 16141 (2005)
19. A. Cao, X. Zhang, C. Xu, J. Liang, D. Wu, B. Wei, J. Mater. Res. **16**, 3107–3110 (2001)
20. P.M. Ajayan, T.W. Ebbesen, T. Ichihashi, S. Iijima, K. Tanigaki, H. Hiura, Nature **362**, 522–525 (1993)
21. K. Hata, D.N. Futaba, K. Mizuno, T. Namai, M. Yumura, S. Iijima, Science **306**, 1362–1364 (2004)

22. R.F. Service, Science **306**, 1275 (2004)
23. H. Ago, N. Uehara, N. Yoshihara, M. Tsuji, M. Yumura, N. Tomonaga, T. Setoguchi, Carbon **44**, 2912–2918 (2006)
24. M. Bystrzejewski, R. Schonfelder, G. Cuniberti, H. Lange, A. Huczko, T. Gemming, T. Pichler, B. Buchner, M. Rummeli, Chem. Mater. **20**, 6586–6588 (2008)
25. A. Peigney, Ch. Laurent, A. Rousset, J. Mater. Chem. **9**, 1167–1177 (1999)
26. A.R. Biris, Z. Li, E. Dervishi, D. Lupu, Y. Xu, V. Saini, F. Watanabe, A.S. Biris, Phys. Lett. A **372**, 3051–3057 (2008)
27. P. Ayala, A.G.T. Gemming, B. Büchner, M.H. Rümmeli, D. Grimm, J. Schumann, R. Kaltofen, F.L. Freire Jr., H.D. Fonseca Filho, T. Pichler, Chem. Mater. **19**, 6131–6137 (2007)
28. M.H. Rümmeli, E. Borowiak-Palen, T. Gemming, T. Pichler, M. Knupfer, M. Kalbác, L. Dunsch, O. Jost, S.R.P. Silva, W. Pompe, B. Büchner, Nano Lett. **5**, 1209–1215 (2005)
29. S.H. Kim, M.R. Zachariah, Mater. Lett. **61**, 2079 (2007)
30. M.H. Rümmeli, F. Schffel, C. Kramberger, T. Gemming, A. Bachmatiuk, R.J. Kalenczuk, B. Rellinghaus, B. Bchner, T. Pichler, J. Am. Chem. Soc. **129**, 15772–15773 (2007)
31. Y.Y. Wei, G. Eres, V.I. Merkulov, D.H. Lowndes, Appl. Phys. Lett. **78**, 1394–1396 (2001)
32. E. Terrado, E. Muñoz, W.K. Maser, A.M. Benito, M.T. Martínez, Diam. Relat. Mater. **16**, 1082–1086 (2007)
33. S. Kir, Y. Selamet, to be published
34. H. Dai, Phys. World **13**, 43–47 (2000)
35. N.Q. Zhao, C.N. He, X.W. Du, C.S. Shi, J.J. Li, L. Cui, Carbon **44**, 1859–1862 (2006)
36. C.J. Lee, J. Park, Y. Huh, Y. Lee, Chem. Phys. Lett. **343**, 33–38 (2001)
37. J. Height, J.B. Howard, J.W. Tester, J.B. Vander Sande, J. Phys. Chem. B **109**, 12337–12346 (2005)
38. A. Datye, Q. Xu, K. Kharas, J. McCarty, Catal. Today **111**, 59–67 (2006)
39. J. Kong, H.T. Soh, A.M. Cassell, C.F. Quate, H. Dai, Nature **395**, 878–881 (1998)
40. X. Li, X. Zhang, L. Ci, R. Shah, C. Wolfe, S. Kar, S. Talapatra, P.M. Ajayan, Nanotechnology **19**, 455609 (2008)
41. M.P. Siegal, D.L. Overmyer, P.P. Provencio, Appl. Phys. Lett. **80**, 2171–2173 (2002)
42. A. Moisala, A.G. Nasibulin, E.I. Kauppinen, J. Phys., Condens. Matter **15**, S3011–S3035 (2003)
43. A.M. Cassell, J.A. Raymakers, J. Kong, H. Dai, J. Phys. Chem. B **103**, 6484–6492 (1999)
44. J. Kong, A.M. Cassell, H. Dai, Chem. Phys. Lett. **292**, 567–574 (1998)
45. S. Kang, K. Cho, K. Kim, G. Cho, J. Alloys Compd. **449**, 269–273 (2008)
46. A.J. Hart, A.H. Slocum, I. Royer, Carbon **44**, 348–359 (2006)
47. O.A. Nerushev, M. Sveningsson, L.K.L. Falk, F. Rohmund, J. Mater. Chem. **11**, 1122–1132 (2001)
48. U.C. Chung, Bull. Korean Chem. Soc. **25**, 1521–1524 (2004)
49. H. Ago, K. Nakamura, N. Uehara, M. Tsuji, J. Phys. Chem. B **108**, 18908–18915 (2004)
50. A.C. Dillon, P.A. Parilla, J.L. Alleman, T. Gennett, K.M. Jones, M.J. Heben, Chem. Phys. Lett. **401**, 522–528 (2005)